Praseodymium-doped cadmium tungstate (CdWO$_4$) nanoparticles for dye degradation with sonocatalytic process

Shahin Ahmadi [a], Abbas Rahdar [b,*], Chinenye Adaobi Igwegbe [c], Sobhan Mortazavi-Derazkola [d], Artur Marek Banach [e], Somayeh Rahdar [a], Ajaya Kumar Singh [f], Susana Rodriguez-Couto [g], George Z. Kyzas [h,*]

[a] Department of Environmental Health, Zabol University of Medical Sciences, Zabol, Iran
[b] Department of Physics, University of Zabol, Zabol, Iran
[c] Department of Chemical Engineering, Namdi Azikiwe University, Awka, Nigeria
[d] Medical Toxicology and Drug Abuse Research Center (MTDRC), Birjand University of Medical Science Birjand, Iran
[e] Department of Biology and Biotechnology of Microorganisms, The John Paul II Catholic University of Lublin, Lublin, Poland
[f] Department of Chemistry, Government V.Y.T.PG. Autonomous College Durg, Chhattisgarh 491001, India
[g] Avenida de Castelao 13, 36209 Vigo, Spain
[h] Department of Chemistry, International Hellenic University, 65404 Kavala, Greece

ARTICLE INFO

ABSTRACT

In the present work, praseodymium-doped cadmium tungstate (Pr-CdWO$_4$) nanoparticles were synthesized, characterized and used as catalysts in a sonocatalytic process to degrade the toxic synthetic azo dye Remazol Black B (RBB). RBB was degraded by 93.9% operating at optimal conditions (pH = 3, C = 100 mg/L, catalyst dosage = 0.35 g/L, T = 298 K and irradiation time 100 min) under an ultrasonic bath at 60 kHz. Further, the addition of different radical scavengers and enhancers to the reaction was assessed. It was found that the addition of the radical scavengers sodium sulfate, sodium carbonate, and sodium chloride decreased RBB degradation from 93.9% to 86.0%, 78.0%, and 71.2%, respectively. On the contrary, the addition of the enhancers potassium periodate, peroxydisulfate and hydrogen peroxide slightly increased the RBB degradation from 93.9% to 95.3%, 96.1%, and 98.7%, respectively. The sonocatalytic process resulted in higher RBB degradation than by applying separately sonolysis (34.7%) and the catalyst as an adsorbent (39.5%). The experimental data followed both the pseudo-first-order (PFO) and Langmuir-Hinshelwood (L-H) kinetics models. However, the PFO gave better fitting (R^2 = 0.993) than the L-H kinetic model (R^2 = 0.9025) at the same optimum experimental conditions. The obtained results pointed out the sonocatalytic process with Pr-doped CdWO$_4$ nanoparticles as a promising process for the degradation of azo dyes and other hazardous organic compounds existing in wastewater.

1. Introduction

Advanced oxidation processes (AOPs) are appealing methods for removing pollutants from wastewater because of their simplicity and high efficiency on the removal of resistant contaminants [1–5]. AOPs are processes involving in situ generation of different reactive oxygen species (ROS) in solution by diverse processes such as sonolysis, ozonation, UV and Fenton processes. These ROS are highly reactive and thus, they are able to oxidize organic compounds non-selectively in a short time period [6]. Among the above-mentioned AOPs, sonolysis has attracted the interest of many researchers because of its environmental friendliness, low cost and lack of sludge generation [1]. The sonolysis process is produced by passing ultrasonic waves as a source of high energy to initiate the formation of acoustic cavitation through a liquid, and the process is also known as acoustic cavitation or ultrasonication. In this process, bubble collisions release a large amount of energy forming hydroxyl (˙OH) and hydrogen radicals (˙H) by the thermal dissociation of water and oxygen [1]. These radicals can oxidize dissolved recalcitrant compounds generating hydrogen peroxide (H$_2$O$_2$). However, the use of only ultrasound waves (sonolysis) to treat wastewater consumes time and a high amount of electrical energy [7]. Also, the application of sonolysis leads to a low degradation rate of organic contaminants and, in addition to this, total degradation rarely takes place [8].

To overcome the above-mentioned limitations, the use of adequate catalysts in sonolysis, such as solid semiconductors, is used. The catalysts provide nucleation sites for cavitation bubbles decreasing the threshold of the ultrasound irradiation intensity required for cavitation to occur. This increases cavitation which in turn increases the generation of hydroxyl radicals and thereby enhancing the degradation of organic pollutants [1]. In addition, some nanoparticles as catalysts in sonolysis can be used to reduce the energy and time for organic pollutant degradation when sonolysis is used separately [1]. These acoustic cavitations may damage the surface of the catalyst and impede agglomeration, thereby decreasing its particle size which will increase the surface area accessible for successive reaction [9]. The addition of catalyst will improve the H_2O_2 molecules dissociation reaction and enhance the quantity of free radicals created for pollutant degradation [9].

Synthetic dyes are one of the most important hazardous compounds [10–18] found in industrial effluents which need to be removed before being discharged into the environment [19]. Among them, azo dyes are the most widely used due to their ease and versatility of synthesis, high dyeing power, and stability [20]. Consequently, they are the most frequently found in industrial effluents. Azo dyes account for 70% of the total world manufactured dyes [21]. They are characterized for the presence of at least one azo group ($—N=N—$) linked to phenyl and naphthyl radicals, which usually contain some functional groups such as amino ($—NH_2$), chlorine ($—Cl$), hydroxyl ($—OH$), methyl ($—CH_3$), nitro ($—NO_2$), sulfonic acid and sodium salts ($—SO_3Na$). Due to the presence of these functional groups, they are hardly decomposed in the natural environment and have toxic, mutagenic and carcinogenic effects [20]. Therefore, azo dyes must be removed from wastewater before being discharged into the water bodies [22–26]. For this reason, the dye degradation is very popular in recent literature [13–15,27–32].

In the present study, Remazol Black B (RBB) was used as a model pollutant (azo dye) to investigate the sonocatalytic degradation potential of the synthesized Pr-CdWO$_4$ nanoparticles as sonocatalysts. Reactive Black B dye has been used in the textile industries for the dying of cotton, woolen and nylon fabrics worldwide. It is reported to be toxic and cause allergic reactions of respiratory tract [33]. The technology "Dye Clean" became a reference in the textile chemistry world market, consisting of dyeing cellulosic fibers with reactive dyes, such as Reactive Black B. This dye is highly soluble in water and difficult to degrade due to its polyaromatic nature [34]. Another troubling fact is the production of aromatic amines due to the degradation of this dye with azo bonds, which are highly carcinogenic [35], while also being considered highly recalcitrant, toxic and mutagenic substances for various aquatic species [36].

These nanoparticles were selected to perform the present study since cadmium tungstate (CdWO$_4$) nanoparticles are known to have optical, magnetic, and electronic properties [37]. Metal tungstate is an extremely significant group of metallic oxides that have found applications in different areas including catalysis, optical fibers, humidity sensors, microwave purposes, etc [38]. CdWO$_4$ nanoparticles were doped with praseodymium (Pr) to increase their electrical conductivity which in turn will enhance the sonoactivity of the CdWO$_4$ nanoparticles (that is extra cavitation and increased generation of hydroxyl radicals) [39]. Although the cost of rare earth metals (industrial vitamins) such as praseodymium (the third member of the lanthanide series) are costly in terms of mining, processing and usage [40] they present significant chemical, optical, magnetic, and electronic properties [41]. These properties are stringent for sonocatalytic processes. A reasonable number of research has not been done on the environmental effects of the use of rareearth metals. Rare earth metals have been used for drugs manufacturing, crop improvement and livestock-feed production.

Even, some rare earth elements nanoparticles are used to treat intractable ailments [42]. To the best of the out knowledge, the application of Pr-CdWO$_4$ nanoparticles as catalysts in a sonocatalytic process to degrade specifically RBB has not been reported previously.
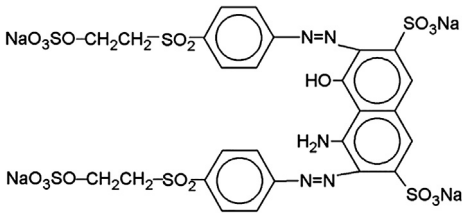
2. Materials and methods

2.1. Materials

The textile dye Remazol Black B (RBB) (Table 1) was purchased from Alvan Sabet Corporation, Hamadan, Iran. All reagents (NaOH 98% and H_2SO_4 99.99%) were of analytical grade and purchased from Merck (Germany). All solutions were prepared using deionized water. All chemicals used for the synthesis of nanoparticles, cadmium nitrate tetrahydrate ($Cd(NO_3)_2 \cdot 6H_2O$, 98%), ethanol (CH_3CH_2OH, 96%), maltose monohydrate ($C_{12}H_{22}O_{11} \cdot H_2O$, 99%), praseodymium(III) nitrate hexahydrate ($Pr(NO_3)_3 \cdot 6H_2O$, 99.9%), sodium tungstate dehydrate ($Na_2WO_4 \cdot 2H_2O$, 99%), were of analytical grade and procured from Sigma-Aldrich, Germany. The pH of the solutions was adjusted using micro-additions of HCl 0.1 N or NaOH 0.1 N.

2.2. Synthesis of Pr-doped CdWO$_4$ nanoparticles

For the preparation of the nanoparticles, maltose was used as a capping agent. Firstly, 0.3 mol of $Cd(NO_3)_2 \cdot 6H_2O$ were dissolved in 20 mL of ethanol. Then, 0.2 M maltose solution was added and stirred vigorously (solution 1). Afterwards, an appropriate amount of $Pr(NO_3)_3 \cdot 6H_2O$ (molar ratio of 1%) was dissolved in solution 1 under ultrasonic waves for 20 min so as to get the solution 2. Next, 0.2 M of $Na_2WO_4 \cdot 2H_2O$ (previously dissolved in 20 mL of distilled water) solution was prepared under continuous stirring (solution 3). The solutions 2 and 3 were then mixed for 15 min to obtain solution 4. Finally, solution 4 was centrifuged and washed with distilled water and ethanol in a Soxhlet apparatus for 12 h and dried in an oven for 3 h at 70 °C. The dried sample was calcinated at 550 °C for 3 h. The resulting nanoparticles were stored at 40 °C.

Table 1
Characteristics and chemical structure of Remazol Black B.

Molecular formula	$C_{26}H_{21}N_5O_{19}S_6Na_4$
Molecular weight	991.82 g/mol
λ_{max}	590 nm
Color index name	C.I. Reactive Black 5
Color index number	C.I. 20,505
Synonyms	Reactive Black 5; Reactive Black B; Remazol Black 5; Remazol Black B; Drimaren Black R/K-3B
Class	Diazo dye
Chemical structure	
Application textile	Cotton
CAS registry number	17095–24-8

2.3. Characterization of the synthesized Pr-CdWO$_4$

To evaluate/characterize the sonocatalyst used in the sonocatalytic degradation of RBB, its properties were determined. Field Emission scanning electron microscopy (FESEM) was used to examine the morphological structure of the Pr-CdWO$_4$ nanoparticles using an LEO instrument, model 1455VP. Fourier transform infrared spectroscopy (FTIR) was applied to determine the functional groups participating in the catalytic process for the degradation of RBB. The FTIR experiments were performed to confirm that the chemical groups on the Pr-CdWO$_4$ nanoparticles were involved in the sonocatalytic degradation of RBB. The FTIR spectra of the catalysts before and after RBB degradation were acquired using a Nicolet Magna 550 spectrometer with a scan range from 400 to 4000 cm^{-1}. The point of zero charge (pH$_{ZPC}$) for Pr-CdWO$_4$ nanoparticles was also determined [1].

2.4. Sonocatalytic experiments

The sonocatalytic experiments (3 repetitions) were performed in an ultrasonic bath operated at an ultrasonic frequency of 60 kHz and an output power of 500 W. Especially, a reactor with a known surface area was used for the pilot test. The reactor was a digital ultrasonic apparatus (Elma CD-Germany, 4820) made from Plexiglas. It had 3.7 L capacity in volume with a 2.5 W/cm^2 per unit of energy input and a power input of 500 W per 100 mL samples in the bath with US waves. The tests were performed inside a closed reactor and there was no contact with the atmosphere that affected the atmospheric gases.

A known mass of catalyst (Pr-CdWO$_4$ nanoparticles) was added to 100 mL of dye solution (fixed concentration). The solution was stirred on a shaker for a specific time (equilibrium at 90 min) in the dark to establish the adsorption–desorption equilibrium. The effect of different operating parameters such as the initial pH of the solution (from 3 to 8), the dosage of Pr-CdWO$_4$ catalyst (from 0.005 to 0.45 g/L), the initial dye concentration (from 50 to 250 mg/L), the temperature (from 298 to 318 K) and the reaction time (from 0 to 100 min) on RBB degradation was studied to determine the optimum conditions required for the optimal degradation of RBB using the sonocatalytic process via Pr-CdWO$_4$ nanoparticles. The optimum pH was determined at a fixed dye concentration of 100 mg/L, a constant Pr-CdWO$_4$ dosage of 0.15 g/L and a temperature of 298 K for different irradiation times. Then, the optimum catalyst dosage was determined at the obtained optimum pH, dye concentration of 100 mg/L and temperature of 298 K for different irradiation times. Subsequently, the initial dye concentration and temperature were optimized. After the treatment, the residual dye concentration was determined using a spectrophotometer (Shimadzu Model: CE-1021-UK) and the degradation efficiency (DE%) was evaluated as follows [43]:

$$DE = \frac{C_0 - C_e}{C_0} \cdot 100\%$$ (1)

where C_0 (mg/L) and C_e (mg/L) are the initial and residual RBB concentrations at time t = 0 and at time t = t, respectively.

Further, the effect of the radical scavengers viz. sodium sulfate (Na$_2$SO$_4$), sodium carbonate (Na$_2$CO$_3$), and sodium chloride (NaCl) at 10 mg/L and the effect of using hydrogen peroxide (H$_2$O$_2$), peroxydisulfate (K$_2$S$_2$O$_8$) and potassium periodate (KIO$_4$) as enhancers at 10 mg/L (based on preliminary studies and a common value used in this type of experiments) on the degradation of RBB were determined at the optimal conditions determined previously at different times (0–100 min) to observe the influence of the presence of different types of scavengers and enhancers on the RBB sonocatalytic degradation process considered via the catalyst, Pr-CdWO4

nanoparticles. The activation energy of the reaction was calculated according to the Arrhenius equation (Eq. (2)) [44]:

$$k = k_0 \cdot e^{-\left(\frac{E_a}{RT}\right)}$$ (2)

where k_0 is the frequency factor and has the same units as k (s^{-1}), E_a is the activation energy (J/mol), R is the universal gas constant (8.314 J/K mol) and T is the temperature (K).

The rate of RBB degradation was analyzed using two kinetics models: the pseudo-first-order (PFO) kinetics equation (Eq. (3)) [43] and the Langmuir-Hinshelwood (Eq. (4)) [45].

$$\ln\left(\frac{C_0}{C}\right) = -k_{app} \cdot t$$ (3)

where C_0 and C are the initial concentration at time t = 0 and the residual dye concentration at time t = t, respectively, k_{app} is the apparent PFO constant, which is obtained from the slope of $\ln(C_0/C)$ versus t, and t is the reaction time (min).

$$\frac{1}{k_{app}} = \frac{1}{k_1 \cdot k_2} + \frac{C_0}{k_1}$$ (4)

where C_0 is the initial dye concentration (mg/L), k_1 is the surface reaction rate constant (mg L^{-1} min^{-1}), k_2 is the Langmuir-Hinshelwood adsorption equilibrium constant (L mg^{-1}) and k_{app} (min^{-1}) is the pseudo-first-order kinetic rate constant.

3. Results and discussion

3.1. Characterization of Pr-CdWO$_4$ nanoparticles

According to the FESEM images shown in Fig. 1, the synthesized Pr-CdWO$_4$ nanoparticles were spherical and had a particle size of about 80–90 nm indicating that it is a nanosized particle. They were distributed forming groups of agglomerated nanoparticles. The gravity of the acoustic cavitation of the catalyst's surface is intensely influenced by the catalyst's size [9]. This particle size will decrease further after cavitation which will increase the catalyst's surface area accessible for the RBB degradation reaction.

The FTIR spectra of the nanoparticles before and after RBB degradation are shown in Fig. 2. The FTIR spectrum of the Pr-CdWO$_4$ nanoparticles before dye degradation indicated the presence of alkyl halides (C—Br stretching) and primary amines (R-N—H$_2$ bending) as shown by the bands at 550 and 1639 cm^{-1}, respectively. A weak peak at 2022 cm^{-1} was also observed which could be assigned to alkynes (—C≡C—) stretching. The broad peak at 3451 cm^{-1} was attributed to O—H stretching of alcohols or phenols. This strong band (O—H stretching) took an active part in the sonocatalytic process for the degradation of RBB. After RBB degradation, the intensities of the bands shifted from 550 and 1639 to 490 cm^{-1} and 1638 cm^{-1}, respectively, and the band at 2022 increased to 2070 cm^{-1}. The intensity of the O—H band shifted from 3451 to 3452 cm^{-1} after the sonocatalytic degradation of RBB, which could be due to the production of ·OH in the process.

3.2. Effect of the initial pH

In the catalytic processes, the pH of the solution affects the catalyst's surface according to its point of zero charge (pH$_{PZC}$) and, thus, the whole process. RBB is an anionic dye, so it is negatively charged when dissociated in water. The effect of pH on the sonocatalytic degradation of RBB was investigated by varying the pH from 3 to 8. It is widely known that the pH plays a basic role in this process, so it is mandatory to start from this factor and then change all the other parameters. However, in the majority of studies, the pH-effect experiments were carried out from pH = 3 (acidic conditions as starting pH point). So, in the present study, it was selected
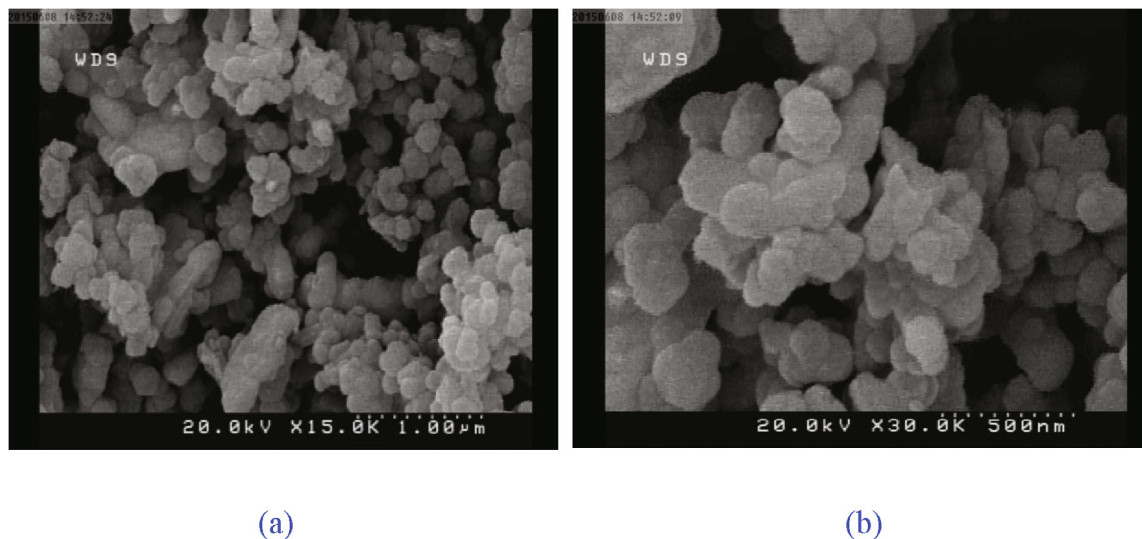
(a)

(b)

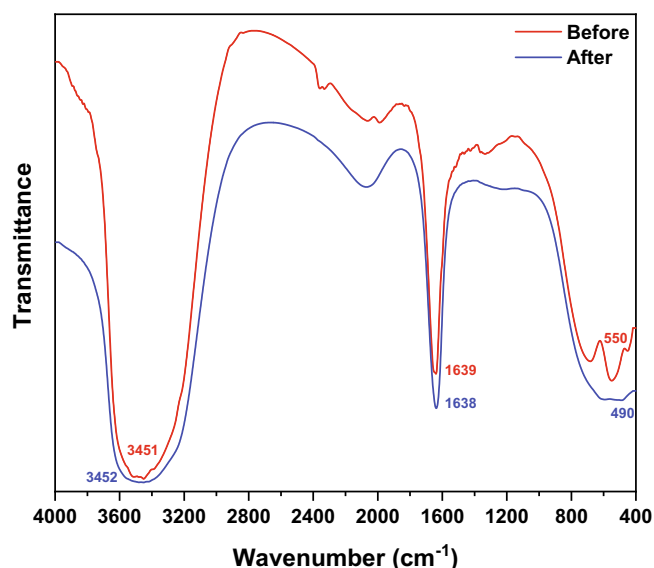**Fig. 1.** FE-SEM images of Pr-CdWO$_4$ nanoparticles at a magnification of (a) 30 × and (b) 15 × .

Fig. 2. FTIR spectra of Pr-CdWO$_4$ nanoparticles before and after RBB degradation.

Fig. 3. Effect of pH on the degradation efficiency of RBB; reaction kinetics at different pH values (experimental conditions: C_0 = 100 mg/L, catalyst dosage = 0.15 g/L, T = 298 K).

this pH value as the first (starting) value. Also, usually the pH-behavior of the process is the same at pH 3 and 4, so we then tested the milder pH acidic conditions (5, 6), the crucial neutral conditions and lastly the mild alkaline conditions (pH = 8). An optimum pH = 3 was found as it can be seen in Fig. 3. The pH$_{PZC}$ value for Pr-CdWO$_4$ was determined to be 4.9 [1]. When the pH of the solution was higher than the pH$_{PZC}$ of the catalyst (i.e. pH$_{PZC}$ > 4.9), the catalyst's surface become negatively charged and the anionic RBB molecules were electrostatically repulsed and thus, the active sites on the catalyst's surface were weak to produce OH radicals and consequently the sonocatalytic RBB degradation decreased. On the contrary, at pH values lower than the pH$_{PZC}$ of the adsorbent (i.e. <4.9), the surface of the catalyst was positively charged and the anionic RBB molecules were electrostatically attracted and thus, the active sites on the catalyst's surface were free for the production of OH radicals resulting in the increase in the sonocatalytic RBB degradation [44,45]. The pKa values for the dye were almost close to 3.8 and 6.9. Therefore, there was an attraction between the surface of the nanocomposite and the dye molecule through the sulfonate group at acidic pH. This resulted in the adsorption
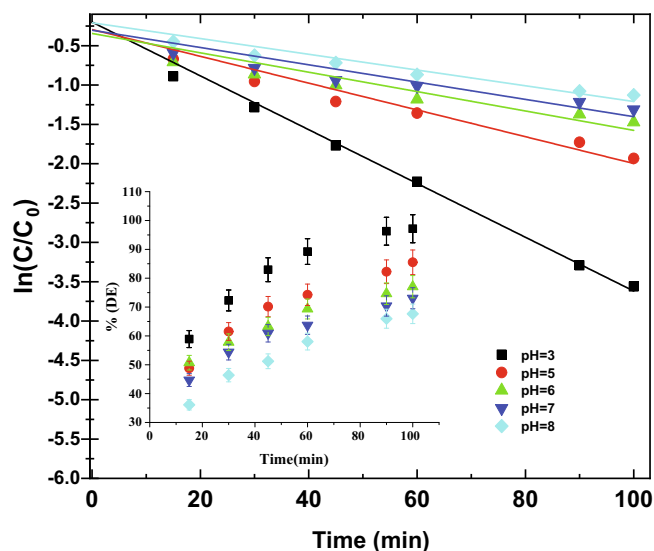
of dye molecules onto the surface and consequently its degradation by the hydroxyl radicals produced by the catalyst. This resulted in the adsorption of dye molecules onto the surface and consequently its degradation with the hydroxyl radicals produced by the catalyst in acid pH [46,47].

The kinetic rate constants (k_{app}) of RBB removal with their correlation coefficients (R^2) at pH values of 3, 5, 6, 7, and 8 are presented in Table 2. The value of k_{app} decreased with increasing pH since the surface properties of the catalyst were changed negatively and the sonocatalytic process was slowed down with increasing pH since increasing the pH resulted in lower generation of OH radicals due to the electrostatic repulsion between the negatively charged catalyst's surface and the anionic RBB dye.
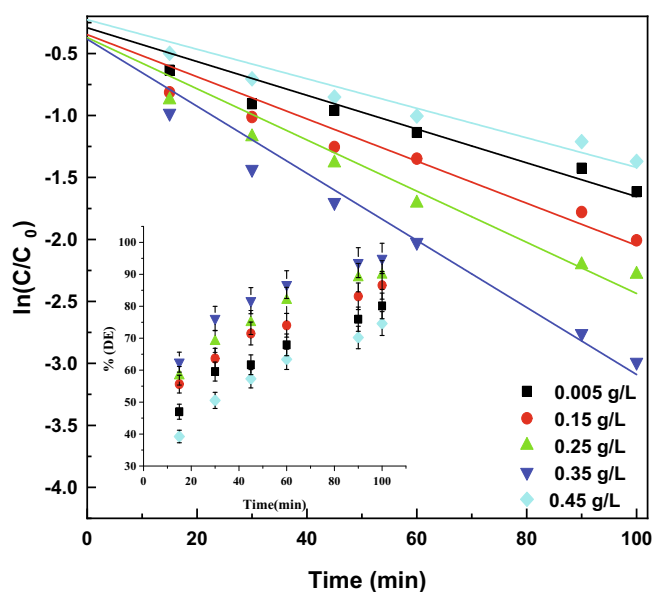
3.3. Effect of catalyst dosage

In Fig. 4, the effect of the catalyst dosage on the catalytic degradation of RBB is shown. As the Pr-CdWO$_4$ dosage increased from

Table 2
Kinetics parameters obtained for the sonocatalytic degradation efficiency of RBB at different pH, concentration, catalyst dosage, and temperature values.
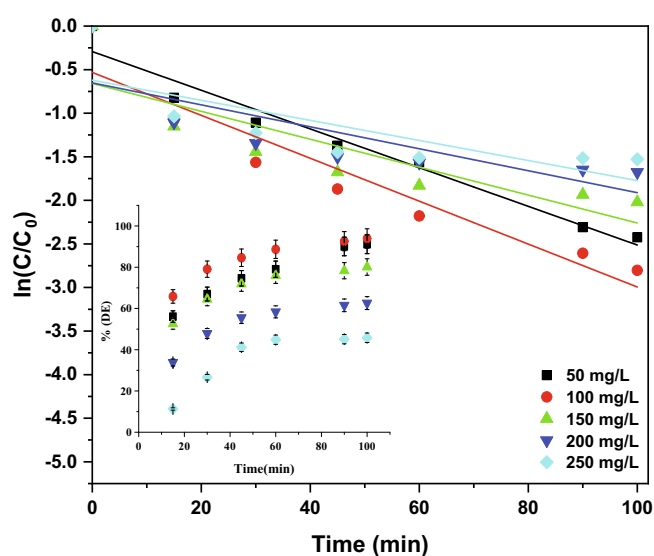
Parameter	pH				
	3	5	6	7	8
k_{app} (min^{-1})	34.2×10^{-3}	17.0×10^{-3}	12.3×10^{-3}	11.0×10^{-3}	10.0×10^{-3}
R^2	0.992	0.938	0.857	0.858	0.913
	Catalyst dosage (g/L)				
	0.005	0.15	0.25	0.35	0.45
k_{app} (min^{-1})	13.6×10^{-3}	34.2×10^{-3}	20.6×10^{-3}	27.1×10^{-3}	11.9×10^{-3}
R^2	0.906	0.992	0.935	0.958	0.925
	Dye concentration (mg/L)				
	50	100	150	200	250
k_{app} (min^{-1})	22.2×10^{-3}	27.1×10^{-3}	16.0×10^{-3}	12.6×10^{-3}	11.5×10^{-3}
R^2	0.961	0.958	0.726	0.630	0.604
	Temperature (K)				
	298	303	308	313	318
k_{app} (min^{-1})	27.1×10^{-3}	14.6×10^{-3}	18.0×10^{-3}	9.1×10^{-3}	6.3×10^{-3}
R^2	0.958	0.891	0.919	0.956	0.999

Fig. 4. Effect of catalyst dosage on the degradation efficiency of RBB; reaction kinetics at different catalyst dosages (experimental conditions: C_0 = 100 mg/L, pH = 3, T = 298 K).

Fig. 5. Effect of initial dye concentration on the sonocatalytic degradation efficiency of RBB at different reaction times; reaction kinetics at different initial dye concentrations (experimental conditions: catalyst dosage = 0.35 g/L, pH = 3, T = 298 K).

0.005 to 0.35 g/L, the percentage of RBB degradation increased from 80 to 95%, respectively. Also, the rate constants of RBB removal increased by increasing the catalyst dosage from 0.005 to 0.35 g/L (Table 2) due to there was a larger surface area with active reaction sites for the production of OH radicals. However, dye degradation decreased when the catalyst dosage increased to 0.45 g/L (80.1%) likely due to nanoparticle agglomeration resulting in a decrease of the surface area.

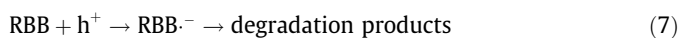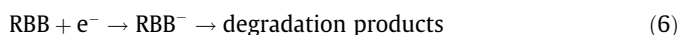### 3.4. Effect of initial dye concentration and reaction time

In Fig. 5, the effect of initial RBB concentration, ranging from 50 to 250 mg/L, on the degradation efficiency was plotted at different reaction times at a constant catalyst dosage of 0.35 g/L, a pH of 3 and a temperature of 298 K. Increase in the concentration of dye from 50 to 100 mg/L caused an amelioration on dye removal due to scavenger reactions of an excess of HO· reacting with themselves. The percentage of RBB degradation decreased from 93.9% to 50.1% when the concentration of RBB increased from 100 to 250 mg/L within 100 min. The rate constants of RBB removal increased up to 100 mg/L and then they decreased (Table 2). The

decrease in RBB degradation was due to the number of OH radicals remained constant but they had to react with more dye molecules. The degradation percentage of RBB also increased with reaction time up to 90 min (equilibrium time) for 50, 100, 150 and 200 mg/L as shown in Fig. 5 and almost became constant from 90 min onwards. The steady-state (or equilibrium) was reached likely due to less or negligible OH radicals being produced with increasing time after the equilibrium time; the limit of OH radicals production had been reached so increasing the time further was not necessary. Similar behavior was previously reported by other researchers. The active sites of the sonocatalyst were also blocked by the anions, which deactivated the sonocatalyst process for degradation of the dye and decreased the DE%. The generation of product intermediate compounds (hydroxyl groups) led to the reduction of the absorbance at high treatment times when the concentration of dye was increased, the limited capacity of the adsorbent checked any further adsorption of the dye, hence the overall removal percentage decreased.

By increasing the dye concentration, the chance of trapping the dye molecule at higher concentrations was less than at lower concentrations. At higher concentrations, most of the composite sites were occupied and the chance of finding available sites for the

adsorption was low. This was the reason for the lower removal percentage at higher concentrations. In addition, for the highest removal under sonication there was an optimum concentration for the pollutant in the mixture. The concentration below and above the optimum concentration can cause a lower effect of cavitation. The dye degradation happened in different ways. Some dye molecules were degraded by hydroxyl radical through oxidation (Eq. (5)) [48]. In addition, several authors have proposed that dye removal occurs through direct electron (e−) transfer from the semiconductor surface to the dye molecule [37,45], as shown by Eq. (6). Direct oxidation by reaction with holes (h+) has also been reported [41], as shown by Eq. (7). Thus, with increasing the dye concentration, it was not possible to degrade 100% of the pollutant as the available species responsible for degradation were approximately constant under the applied conditions.

$$RBB + \cdot OH \rightarrow RBB^{\cdot -} + H_2O \rightarrow \text{degradation products} \quad (5)$$

$$RBB + e^- \rightarrow RBB^- \rightarrow \text{degradation products} \quad (6)$$

$$RBB + h^+ \rightarrow RBB^{\cdot -} \rightarrow \text{degradation products} \quad (7)$$

3.5. Effect of temperature

Along with pH, temperature is also an important parameter in sonocatalysis because it does not only affect the activation energy but also the pollutant behavior. Thus, in this study, kinetics tests of RBB removal by sonocatalysis were conducted at different temperatures (i.e. 298, 303, 308, 313 and 318 K). As a result, the rate constants with their correlation coefficients were determined (Table 2). Nevertheless, the rate constants decreased as the temperature increased (Fig. 6 and Table 2), which was also confirmed by Eq. (2); the degradation rate constant (k) was inversely proportional to temperature (T).

From the plot, ln$k$ versus $1/T$ (Fig. 7), the activation energy (E_a) was calculated and a value of 38.65 kJ mol^{-1} obtained. Also, based on the Eyring equation, the calculated ΔH^0 and ΔG^0 were 4.6496 kJ mol^{-1} and −19.621 J mol^{-1}K^{-1}, respectively. The relationship between ΔG^0 and temperature is denoted as Eq. (8):

$$\Delta G^0 = -4.6496 + 0.019621 \cdot T \quad (8)$$
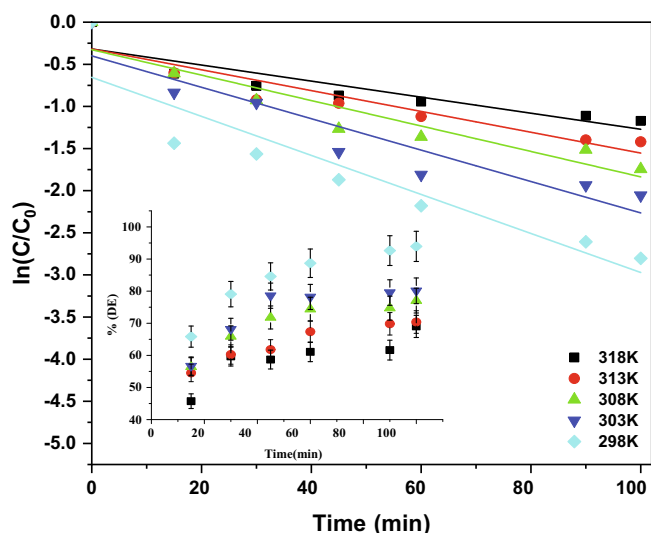

Fig. 6. Effect of temperature on the sonocatalytic degradation efficiency of RBB; reaction kinetics at different temperature values (experimental conditions: C_0 = 100 mg/L, catalyst dosage = 0.35 g/L, pH = 3).
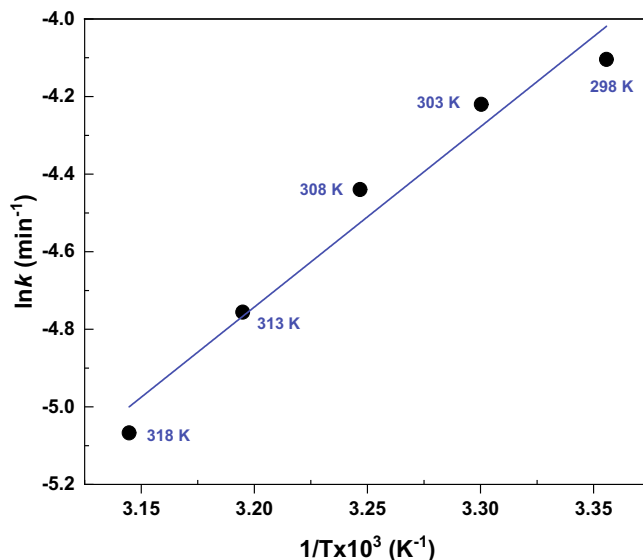

Fig. 7. Arrhenius plot for RBB degradation.

when the temperature increased, ΔG^0 also increased and the reaction rate decreased since an increase in temperature will increase the kinetic energy levels of the pollutant leading to more dispersion of the RBB molecules in water thus preventing its degradation [49].
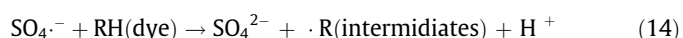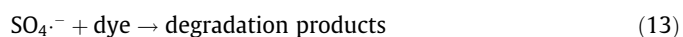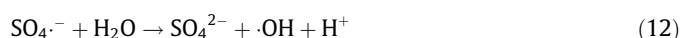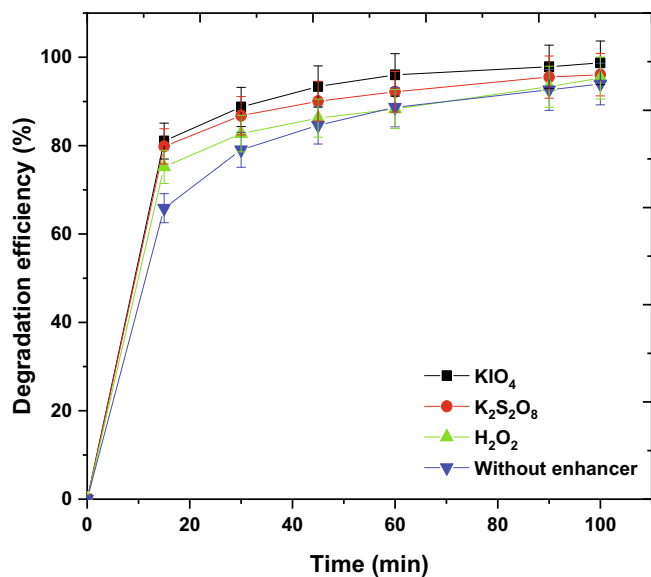
3.6. Effect of enhancers

The impact of the most commonly used enhancers, potassium periodate (KIO$_4$), peroxy disulfate (K$_2$S$_2$O$_8$) and hydrogen peroxide (H$_2$O$_2$) on RBB degradation was examined at 100 mg/L of RBB concentration and an enhancer concentration of 10 mg/L. The addition of the above-mentioned enhancers slightly increased the RBB sonocatalytic degradation from 93.9 to 98.7, 96.1, and 95.3%, respectively (Fig. 8).

To explain this phenomenon, in regard to liquid phase reactions, hydrogen peroxide is an extremely effective oxidant. Ultrasonic irradiation plays a key role in the creation of reactive species (H$_2$O$_2$, ·OH, H·, ·O and ·OOH) [49–51]. The recombination of hydroxyl radicals may generate H$_2$O$_2$ because of the occurrence of cavitation in aqueous solution·H$_2$O$_2$ formation is enhanced by higher intensity ultrasound generation when ultrasonic irradiation exists (Eqs. (9) and (10)). Moreover, the existence of hydrogen peroxide (H$_2$O$_2$) expedites OH radicals' production rate by reduction at conduction band [51]:

$$H_2O_2)))) \rightarrow 2H^0O \quad (9)$$

$$H_2O_2 + e^- \rightarrow \cdot OH + OH^- \quad (10)$$

The addition of peroxydisulfate may also enhance $DE(\%)$ by creating sulfate radicals that produce ·OH when reacted with water (Eqs. (11)–(15)). Since sulfate radicals are highly reactive and one of the strongest oxidants available with an oxidation potential of 2.6 V as compared to ·OH (2.7 V) [50–53]:

$$S_2O_8^{2-}))) \rightarrow 2SO_4^{\cdot -} \quad (11)$$

$$SO_4^{\cdot -} + H_2O \rightarrow SO_4^{2-} + \cdot OH + H^+ \quad (12)$$

$$SO_4^{\cdot -} + \text{dye} \rightarrow \text{degradation products} \quad (13)$$

$$SO_4^{\cdot -} + RH(\text{dye}) \rightarrow SO_4^{2-} + \cdot R(\text{intermidiates}) + H^+ \quad (14)$$

Fig. 8. Effect of enhancers on the sonocatalytic degradation of RBB (catalyst dosage = 0.35 g/L, C_0 = 100 mg/L, enhancer concentration = 10 mg/L, pH = 3, T = 298 K).

$$SO_4 \cdot^- + R(intermidiates) \rightarrow SO_4{}^{2-} + CO_2 + NO_2$$
$$+ \text{other inorganics} \tag{15}$$
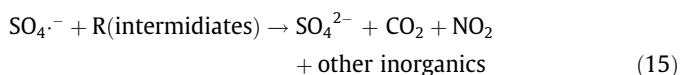
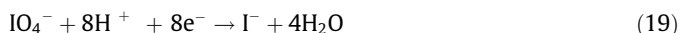Periodate ions may be regarded as instances of the formation of higher reactive secondary radicals. Potassium periodate is more beneficial to $DE(\%)$ when the produced electrons in the conduction band are captured (Eqs. (16)–(19)) [51,53].

$$IO_4^+ \rightarrow IO_3 \cdot + O \cdot^- \tag{16}$$

$$O \cdot^- + H^+ \rightarrow \cdot OH \tag{17}$$

$$\cdot OH + IO_4{}^- \rightarrow OH^- + IO_4 \tag{18}$$

$$IO_4{}^- + 8H^+ + 8e^- \rightarrow I^- + 4H_2O \tag{19}$$

3.7. Effect of radical scavengers

The most commonly studied radical scavengers, sodium chloride (NaCl), sodium carbonate (Na_2CO_3) and sodium sulfate (Na_2SO_4) were selected for this study at a concentration of 10 mg/L. As observed in Fig. 9, all scavengers decreased the sonocatalytic degradation of RBB which proved that the free radical ($\cdot OH$) attack was the main mechanism in the sonocatalytic process. Thus, RBB degradation was highest in the absence of $\cdot OH$ scavenging agents within 100 min (93.9%). Scavengers decreased RBB degradation in the following order: Na_2SO_4 (86.0%) > Na_2CO_3 (78.0%) > NaCl (71.2%). The inhibiting impact of Na_2SO_4, Na_2CO_3 and NaCl on RBB degradation was due to the scavenging of the $\cdot OH$ during the sonocatalytic process. The addition of a scavenger could deactivate the active species involved in the sonocatalytic process and they were not able to react in the process of RBB degradation therefore decreased in sonocatalytic performance. They scavenged the $\cdot OH$ transforming into anionic radicals such as sulfate radicals ($SO_4{}^{2-}$), carbonate radicals ($CO_3{}^{2-}$) and chloride radicals ($\cdot Cl^-$), respectively, which were less efficient [54].
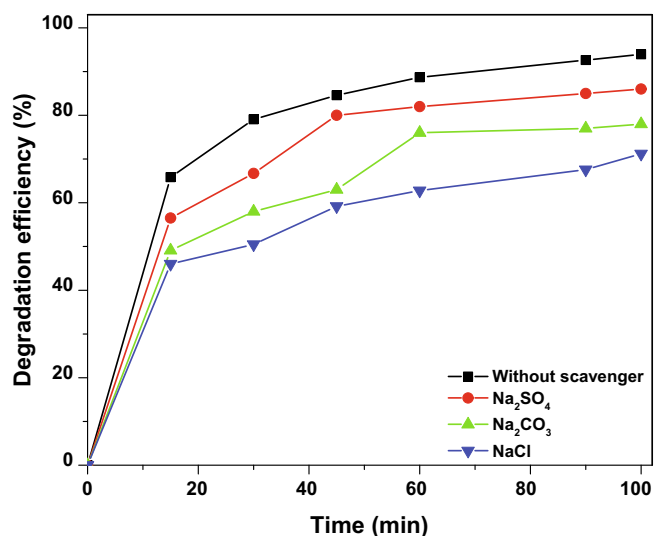

Fig. 9. Sonocatalytic degradation efficiency in the presence of different radical scavengers (catalyst dosage = 0.35 g/L, C_0 = 100 mg/L, scavenger concentration = 10 mg/L, pH = 3, T = 298 K).

3.8. Kinetic modeling of the sonocatalytic process

The sonocatalytic degradation followed the pseudo-first-order kinetics model. The apparent reaction rate constants (k_{app}) were acquired from the slope of the straight-line plot of $\ln(C/C_0)$ against time (t) (Fig. 10) using Eq. (3). The k_{app} and correlation coefficients (R^2) values were obtained as 16.5×10^{-3} min^{-1} and 0.993, respectively. The high R^2 value implies that the sonocatalytic degradation of RBB using Pr-CdWO$_4$ obeyed the PFO kinetics model at the optimal conditions.

The $1/k_{app}$ and C_0 linear relation at optimum conditions (C_0 = 100 mg/L, catalyst dosage = 0.35 g/L, pH = 3, reaction time = 100 min and T = 298 K) using Eq. (4) is presented in Fig. 11. The RBB sonocatalytic degradation process followed the Langmuir–Hinshelwood (L–H) mechanism since the R^2 > 0.900; this model can be used to fit the present study. The surface reaction rate constant (k_1) was obtained as 0.2451 mg/L min. The
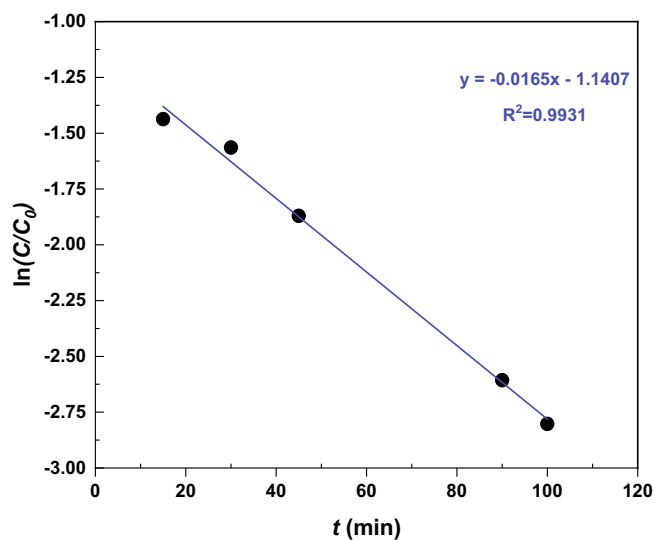
Fig. 10. PFO kinetics for the sonocatalytic degradation of RBB at optimum conditions (C_0 = 100 mg/L, catalyst dosage = 0.35 g/L, pH = 3, reaction time = 100 min) at optimum T = 298 K).
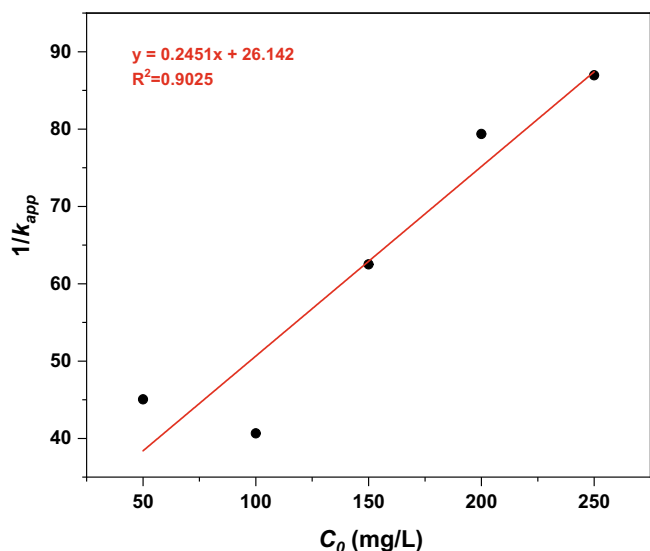
Fig. 11. The relationship between $1/k_{app}$ and the initial concentration of RBB (pH = 3, catalyst dosage = 0.35 g/L, T = 298 K and reaction time = 100 min).

Langmuir–Hinshelwood adsorption equilibrium constant was 0.1561 L/mg. The data fitted better into the PFO kinetics model than the L-H kinetics model at the same experimental conditions (at the optimum).

The earliest photocatalysis papers routinely used Langmuir-Hinshelwood rate forms because photocatalysis is a subfield of heterogeneous catalysis. The latter field has historically been dominated by this analytic function

$$rate = \frac{k_{cat} \cdot K_{ads} \cdot C}{1 + K_{ads} \cdot C} \qquad (20)$$

where k_{cat} is a fundamental representation of catalyst activity, and K_{ads} is, historically, the adsorption equilibrium constant of the Langmuir isotherm,

$$K_{ads} = \frac{k_1}{k_{-1}} \qquad (21)$$

where k_1 and k_{-1} are reactant adsorption and desorption constants, respectively.

In photocatalysis, k_{cat} is the product of a rate constant, k', and some active species such as OH radicals or semiconductor hole concentration, $h+$. Since these active species are the presumed result of photoactivation, their concentrations, and thus the catalytic rate constant, k_{cat}, are expected to be a function of light intensity (I). In contrast, the traditional Langmuir-Hinshelwood approach assuming adsorption/desorption equilibrium contains rate constants k_1 and k_{-1} which are not assumed to depend on intensity. The experimental observation that not only k_{cat}, but also K_{ads}, depended upon intensity indicated failure of the equilibrated adsorption assumption. This situation has been rectified by invoking a pseudo-steady state (PSS) assumption, commonly used in other kinetic analyses involving highly unstable intermediates such as free radicals. This analysis allowed k_{cat} to have any value relative to k_{-1}. In particular, the PSS analysis led to an apparent adsorption constant, K_{ads}, which depended upon k_{cat}, and thus varied with intensity [55]:

$$K_{ads}(apparent) = \frac{k_1}{k_{-1} + k_{cat}} \qquad (22)$$

Because all photocatalyzed aqueous phase oxidations carried out in the presence of water and molecular oxygen produce the same active species, OH and $h+$, we may expect that all such conversions require PSS rather than Langmuir-Hinshelwood analyses.

Although various sonochemical reactions and sonocatalytic degradation have already been reported, the kinetic for the reactions is still unclear in homogeneous and heterogeneous solutions. This is due to simultaneously and consecutively proceeding of the reactions under ultrasound. In the literature, it was reported that the sonochemical and the sonocatalytic dye degradation in liquid media could be described by the first-order kinetic model [50–54].

3.9. Mechanism of sonocatalytic dye degradation

The degradation of RBB (for an initial concentration of 100 mg/L) was compared under ultrasonic irradiation in the presence of Pr-CdWO$_4$ nanoparticles (i.e. sonocatalysis) and absence of Pr-CdWO$_4$ nanoparticles (i.e. sonolysis) under the same operational conditions (i.e. catalyst dosage = 0.35 g/L, C_0 = 100 mg/L, pH = 3, T = 298 K) for 100 min of treatment (Fig. 12). Also, using only the Pr-CdWO$_4$ nanoparticles as an adsorbent in the absence of ultrasonic irradiation was considered. An RBB degradation of 39.5% and 34.8% were obtained using adsorption and sonolysis, respectively. Using Pr-CdWO$_4$ nanoparticles under ultrasonic irradiation (i.e. sonocatalysis), an RBB degradation of 93.9% was achieved within 100 min. This improvement was associated with the combination of ultrasonic irradiation and Pr-CdWO$_4$ nanoparticles which increased ·OH production. Thus, the presence of an heterogeneous catalyst enhanced the formation rate of cavitation bubbles by providing nucleation sites which in turn enhanced the generation of free radicals [56]:

3.10. Comparison of sonolysis, adsorption and sonocatalysis processes for the RBB degradation

The sonocatalytic degradation mechanism of RBB using Pr-CdWO$_4$ as a catalyst is presented in Fig. 13. Upon the irradiation of Pr-CdWO$_4$ by ultrasonic waves, photo-generated electrons were excited from the Pr-CdWO$_4$ valence band. When the electrons reacted with O$_2$, O$_2^-$ was generated and ·OH was generated when the cavities were formed in water and their subsequent collapse, which may generate immense local temperature and pressure rising usually up to 5000 K, pressure of 1000 atm [45,57]. Under the generated heat excitation, electrons were transferred from the Pr-CdWO$_4$ valence band (VB) to the conduction band (CB). Then, electron-hole pairs were created at the inner or surface of Pr-CdWO$_4$ nanoparticles. The generated valence band holes were able to directly disintegrate the RBB at the Pr-CdWO$_4$nanoparticles'
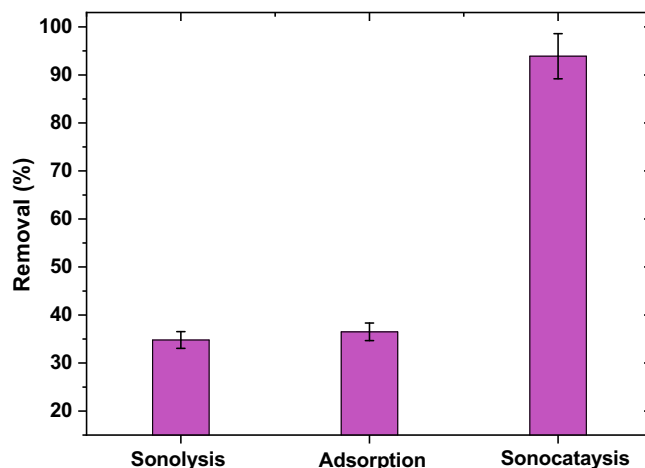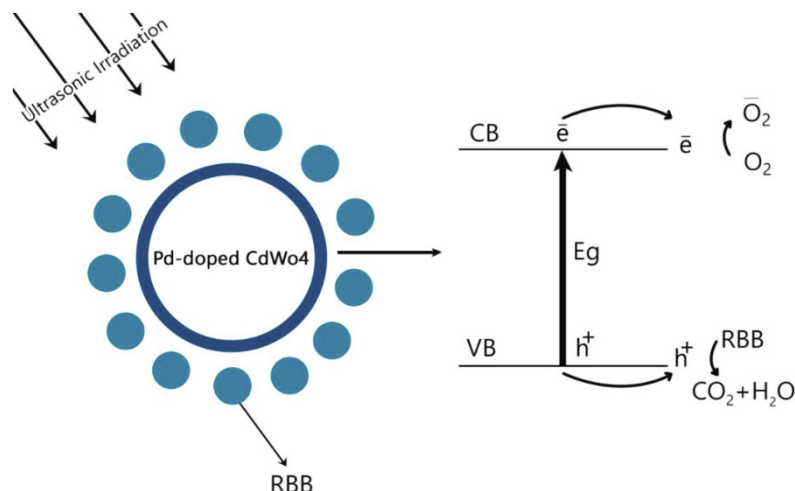

Fig. 12. Comparison of different processes on the degradation of RBB (C_0 = 100 mg/L, catalyst dosage = 0.35 g/L, T = 298 K and reaction time = 100 min, pH = 3).

Fig. 13. Sonocatalytic degradation of RBB in the presence of Pr-CdWO$_4$ nanoparticles under ultrasonic irradiation.

surface until complete degradation occurred. Also, the generated holes reacted with the H$_2$O molecules to produce hydroxyl radicals (·OH) on the Pr-CdWO$_4$ nanoparticles' surface which subsequently degraded RBB in the aqueous solution. Concurrently, the generated electrons reacted with O$_2$ dissolved within the bulk solution and created super oxygen radical anions (O$_2^-$) that turned into hydroxyl radicals (·OH) *via* numerous chemical reactions [56].

Today, from various methods, AOPs are considered auspicious treatments to remove various recalcitrant dyes such as RBB. Based on Table 3, numerous researchers have examined RBB removal in aqueous environments *via* several AOPs and other processes including adsorption, electrochemical, and biodegradation methods. Compared to prior studies (Table 3), the sonocatalytic process is a favourable method for the removal of RBB. In addition to suitable removal efficiency, other benefits include its moderate costs and non-toxicity. However, the majority of the results in Table 3

are better than that of the present study. Nonetheless, this process is better than: (i) the Fenton process, since it involves the constant addition of reagents, (ii) the biodegradation method because using microorganisms is cumbersome and the degradation times are long, (iii) the adsorption technique, which requires the disposal of the desorbed pollutant and adsorbent disposal, (iv) the electro-coagulation process, which requires high power consumption. In addition, a new catalyst that can be used for sonocatalytic processes was obtained but more studies are required in order to make this process a feasible option.

Nowadays, among different methods, AOPs are a promising treatment for the removal of different dyes (Table 4). In comparison to other studies (Table 4), the sonocatalytic process is an effective method for the removal of RBB; in addition to the good removal efficiency, the other benefits of this method suchas moderate cost, non-toxicity and aqueous solubility make this method more suitable.

4. Conclusions

The applicability of Pr-CdWO$_4$ nanoparticles for the degradation of RBB from aqueous solution using a sonocatalytic process was examined. A maximum RBB degradation of 93.9% was obtained operating at a pH of 3, a Pr-doped CdWO$_4$ dosage of 0.35 g/L, an RBB concentration of 100 mg/L, a temperature of 298 K, an irradiation time of 100 min and an ultrasonic frequency of 60 kHz. In addition, this degradation percentage was increased up to 98.7% when H$_2$O$_2$ (10 mg/L) was used as an enhancer. The sonocatalytic degradation of RBB obeyed both the pseudo-first-order (PFO) and Langmuir-Hinshelwood (L-H) kinetics models. The sonocatalytic degradation process was shown to have significant potential for the treatment of aqueous solutions containing azo dyes and organic compounds.

Table 3
Removal of Reactive Black B (RBB) from aqueous solutions obtained with different physicochemical and biodegradation treatments.

Process	Concentration (mg/L)	Removal	Ref.
Adsorption (activated carbon fromBrazilian-pine fruit shell)	100	94% in 4 h	[58]
Electrocoagulation (Fe)	5000	96.0% in 80 min	[59]
Electrocoagulation (Al)	5000	89.4% in 80 min	[59]
Adsorption using bagasse	25	95.0% in 15 min	[60]
Biodegradation (*Ganoderma sp.*)	70	89.2% in 7 d	[61]
Biodegradation (*Ganoderma sp.* crude ligninolytic enzymes)	70	90.8% in 7 d	[61]
Biodegradation by extracellular fungal laccase from *Aspergillus oryzae* AM1101	50	76.0% in 45 min	[62]
O$_3$/H$_2$O$_2$	100	98.0% in 25 min	[63]
Fenton process (H$_2$O$_2$/Fe^{+2})	100	99.9% in 5 min	[63]
UV/H$_2$O$_2$	100	99.0% in 15 min	[63]
Adsorption (P-γ-Fe$_2$O$_3$ nanoparticles)	100	99.7% in 10 min	[64]
Sonocatalytic degradation (Pr-CdWO$_4$ nanoparticles as catalyst and H$_2$O$_2$ as the enhancer)	100	98.7% in 100 min	This study

CRediT authorship contribution statement

Shahin Ahmadi: Conceptualization, Investigation, Formal analysis, Methodology, Writing - original draft. **Abbas Rahdar:** Conceptualization, Investigation, Formal analysis, Methodology, Writing - original draft, Supervision. **Chinenye Adaobi Igwegbe:** Conceptualization, Investigation, Formal analysis, Methodology, Writing - original draft. **Sobhan Mortazavi-Derazkola:** Conceptualization, Investigation, Formal analysis, Methodology, Writing - original draft. **Artur Marek Banach:** Conceptualization,

Table 4
Summary of the AOP degradation processes applied in the treatment of dyes.

AOP	Dye	Operational condition	Results	Ref
Sonocatalytic	Acid Blue 92	- Initial dye concentration = 10 mg/L - Catalyst dosage (Sm-doped ZnO) = 1 g/L - Dopant percentage = 6%, - Ultrasonic power = 150 W. - Reaction time = 150 min - Frequency = 36 kHz	DE = 90.10%	[53]
Sonocatalytic	Methyl orange	- Initial dye concentration = 10 mg/L - Catalyst dosage (modified TiO_2) = 1 g/L - Ultrasonic power = 70 W. - Irradiation time = 1 h - Frequency = 20 kHz	DE = 82%	[65]
Sonocatalytic	Rhodamine B	- Initial dye concentration = 5 mg/L - Catalyst dosage (p-TiO_2) = 0.5 g/L - Ultrasonic power = 80 W. - Irradiation time = 2 h - Frequency = 40 kHz - temperature 600 °C - pH = 6	DE = 81%	[66]
Electrochemical	RBB	- current density: 2.5 A/dm^2 - electrolysis duration: 6 h - voltage = 4.9 V	COD removal = 72.9%	[67]

Investigation, Formal analysis, Methodology, Writing - original draft. **Somayeh Rahdar:** Conceptualization, Investigation, Formal analysis, Methodology, Writing - original draft. **Ajaya Kumar Singh:** Conceptualization, Investigation, Formal analysis, Methodology, Writing - original draft. **Susana Rodriguez-Couto:** Conceptualization, Investigation, Formal analysis, Methodology, Writing - original draft, Supervision. **George Z. Kyzas:** Conceptualization, Investigation, Formal analysis, Methodology, Writing - original draft.

Declaration of Competing Interest

The authors declare that they have no known competing financial interests or personal relationships that could have appeared to influence the work reported in this paper.

Acknowledgement

References

[1] S. Rahdar, C. Igwegbe, A. Rahdar, S. Ahmadi, Efficiency of sono-nano-catalytic process of magnesium oxide nanoparticle in removal of penicillin G from aqueous solution, Desalin. Water Treat. 106 (2018) 335.

[2] C.A. Igwegbe, S. Ahmadi, S. Rahdar, A. Ramazani, A.R. Mollazehi, Efficiency comparison of advanced oxidation processes for ciprofloxacin removal from aqueous solutions: chemical, -nano-chemical and -nano-chemical/persulfate process, Environ. Eng. Res. 25 (2020) 178–185.

[3] G. Fang, C. Liu, J. Gao, D.D. Dionysiou, D. Zhou, Manipulation of persistent free radicals in biochar to activate persulfate for contaminant degradation, Environ. Sci. Technol. 49 (9) (2015) 5645–5653.

[4] S. Ye, M. Yan, X. Tan, J. Liang, G. Zeng, H. Wu, B. Song, C. Zhou, Y. Yang, H. Wang, Facile assembled biochar-based nanocomposite with improved graphitization for efficient photocatalytic activity driven by visible light, Appl. Catal. B 250 (2019) 78–88.

[5] S. Ye, G. Zeng, X. Tan, H. Wu, J. Liang, B. Song, N. Tang, P. Zhang, Y. Yang, Q. Chen, X. Li, Nitrogen-doped biochar fiber with graphitization from Boehmeria nivea for promoted peroxymonosulfate activation and non-radical degradation pathways with enhancing electron transfer, Appl. Catal. B 269 (2020) 118850.

[6] C. Ren, B. Yang, M. Wu, J. Xu, Z. Fu, Y. Lv, T. Guo, Y. Zhao, C. Zhu, Synthesis of Ag/ZnO nanorods array with enhanced photocatalytic performance, J. Hazard. Mater. 182 (1) (2010) 123–129.

[7] J. Lifka, B. Ondruschka, J. Hofmann, The Use of Ultrasound for the Degradation of Pollutants in Water: Aquasonolysis – A Review, Engineering in Life Sciences 3 (6) (2003) 253–262.

[8] R.J. Emery, M. Papadaki, L.M. Freitas dos Santos, D. Mantzavinos, Extent of chemical degradation and change of toxicity of a pharmaceutical precursor (triphenylphosphine oxide) in water as a function of treatment conditions, Environ. Int. 31 (2005) 207–211.

[9] Y.L. Pang, A.Z. Abdullah, S. Bhatia, Review on sonochemical methods in the presence of catalysts and chemical additives for treatment of organic pollutants in wastewater, Desalination 277 (1) (2011) 1–14.

[10] J.S. Aguirre-Araque, R.R. Guimaraes, H.E. Toma, Chemistry of ternary monocarboxyterpyridine-bipyridine-trimercaptotriazine ruthenium complexes and application in dye sensitized solar cells, Polyhedron 182 (2020).

[11] K.M. Aiswarya, T. Raguram, K.S. Rajni, Synthesis and characterisation of nickel cobalt sulfide nanoparticles by the solvothermal method for dye-sensitized solar cell applications, Polyhedron 176 (2020).

[12] M.A. Akram, J. Ye, G. Wang, L. Shi, Z. Liu, H. Lu, S. Zhang, G. Ning, Bifunctional chemosensor based on a dye-encapsulated metal-organic framework for highly selective and sensitive detection of $Cr_2O_7^{2-}$ and Fe3+ ions, Polyhedron 185 (2020).

[13] P. Alimard, Fabrication and kinetic study of Nd-Ce doped Fe_3O_4-chitosan nanocomposite as catalyst in Fenton dye degradation, Polyhedron 171 (2019) 98–107.

[14] X. Du, H. He, L. Du, W. Li, Y. Wang, Q. Jiang, L. Yang, J. Zhang, S. Guo, Porous Pr (III)-based organic framework for dye-adsorption and photo degradation with (4,5)-c net, Polyhedron 171 (2019) 221–227.

[15] C. Fan, Z. Zong, X. Zhang, B. Su, Z. Zhu, C. Bi, Y. Fan, Syntheses, structural diversity and photo-degradation and dye adsorption properties of novel Ni(II)/Co(II) coordination polymers modulated by 4-(4-carboxylphenylmethylthio) benzoic acid ligand, Polyhedron 170 (2019) 515–522.

[16] S.G. Ghomshehzadeh, V. Nobakht, N. Pourreza, P. Mercandelli, L. Carlucci, A new pillared Cd-organic framework as adsorbent of organic dyes and as precursor of CdO nanoparticles, Polyhedron 176 (2020).

[17] Q. Hu, Q.M. Zheng, X.R. Ma, Z.Z. Lai, T.Q. Ye, L. Qin, One luminescence probe and the impact of dye-adsorption on the luminescent property, Polyhedron 177 (2020).

[18] X. Liu, C. Hao, L. Cui, Y. Wang, An anionic cadmium-organic framework with an uncommon 3,3,4,8-c network for efficient organic dye separation, Polyhedron 188 (2020).

[19] B. Debnath, A.S. Roy, S. Kapri, S. Bhattacharyya, Efficient dye degradation catalyzed by manganese oxide nanoparticles and the role of cation valence, ChemistrySelect 1 (14) (2016) 4265–4273.

[20] S. Ahmadi, L. Mohammadi, C.A. Igwegbe, S. Rahdar, A.M. Banach, Application of response surface methodology in the degradation of Reactive Blue 19 using H2O2/MgO nanoparticles advanced oxidation process, Int. J. Ind. Chem. 9 (3) (2018) 241–253.

[21] S. Ahmadi, L. Mohammadi, A. Rahdar, S. Rahdar, R. Dehghani, C. Adaobi Igwegbe, G.Z. Kyzas, Acid dye removal from aqueous solution by using neodymium(III) oxide nanoadsorbents, Nanomaterials 10 (3) (2020) 556.

[22] S. Kamal, G.T. Pan, S. Chong, T.C.K. Yang, Ultrasonically induced sulfur-doped carbon nitride/cobalt ferrite nanocomposite for efficient sonocatalytic removal of organic dyes, Processes 8 (1) (2020).

[23] V.T. Pham, H.T.T. Nguyen, D.T.C. Nguyen, H.T.N. Le, T.T. Nguyen, N.T.H. Le, K.T. Lim, T.D. Nguyen, T. Van Tran, L.G. Bach, Process optimization by a response surface methodology for adsorption of Congo red dye onto exfoliated graphite-decorated $MnFe_2O^4$ nanocomposite: the pivotal role of surface chemistry, Processes 7 (5) (2019).

[24] M.Z.M. Salem, I.H.M. Ibrahim, H.M. Ali, H.M. Helmy, Assessment of the use of natural extracted dyes and pancreatin enzyme for dyeing of four natural textiles: HPLC analysis of phytochemicals, Processes 8 (1) (2020).

[25] H. Saroyan, G.Z. Kyzas, E.A. Deliyanni, Effective dye degradation by graphene oxide supported manganese oxide, Processes 7 (1) (2019).

[26] B.S. Trinh, P.T. Le, D. Werner, N.H. Phuong, T.L. Luu, Rice husk biochars modified with magnetized iron oxides and nano zero valent iron for decolorization of dyeing wastewater, Processes 7 (10) (2019).

[27] M.H. Barzegar, M. Ghaedi, V. Madadi Avargani, M.M. Sabzehmeidani, F. Sadeghfar, R. Jannesar, Electrochemical synthesis and efficient photocatalytic degradation of azo dye alizarin yellow R by Cu/CuO nanorods under visible LED light irradiation using experimental design methodology, Polyhedron 158 (2019) 506–514.

[28] C.R. Czarnecki, R.L. LaDuca, Structural diversity and dye degradation capability of copper 1,2-phenylenediacetate coordination polymers with flexible dipyridylamide ligands, Polyhedron 161 (2019) 161–168.

[29] Y.P. Hamedani, M. Hekmati, Green biosynthesis of silver nanoparticles decorated on multi-walled carbon nanotubes using the extract of Pistacia atlantica leaves as a recyclable heterogeneous nanocatalyst for degradation of organic dyes in water, Polyhedron 164 (2019) 1–6.

[30] S. Jalali, M.R. Rahimi, K. Dashtian, M. Ghaedi, S. Mosleh, One step integration of plasmonic Ag$_2$CrO$_4$/Ag/AgCl into HKUST-1-MOF as novel visible-light driven photocatalyst for highly efficient degradation of mixture dyes pollutants: Its photocatalytic mechanism and modeling, Polyhedron 166 (2019) 217–225.

[31] H. Li, Q. Li, X. He, Z. Xu, Y. Wang, L. Jia, Synthesis of AgBr@MOFs nanocomposite and its photocatalytic activity for dye degradation, Polyhedron 165 (2019) 31–37.

[32] L. Wang, T. Zeng, G. Liao, Q. Cheng, Z. Pan, Syntheses, structures and catalytic mechanisms of three new MOFs for aqueous Cr(VI) reduction and dye degradation under UV light, Polyhedron 157 (2019) 152–162.

[33] H. Zollinger, Color Chemistry: Synthesis, Properties and Applications of Organic Dyes and Pigments, 1987.

[34] J. Fan, Y. Guo, J. Wang, M. Fan, Rapid decolorization of azo dye methyl orange in aqueous solution by nanoscale zerovalent iron particles, J. Hazard. Mater. 166 (2–3) (2009) 904–910.

[35] V.J.P. Vilar, L.X. Pinho, A.M.A. Pintor, R.A.R. Boaventura, Treatment of textile wastewaters by solar-driven advanced oxidation processes, Sol. Energy 85 (9) (2011) 1927–1934.

[36] M. Vedrenne, R. Vasquez-Medrano, D. Prato-Garcia, B.A. Frontana-Uribe, M. Hernandez-Esparza, J.M. de Andrés, A ferrous oxalate mediated photo-Fenton system: toward an increased biodegradability of indigo dyed wastewaters, J. Hazard. Mater. 243 (2012) 292–301.

[37] B. Fatima, S.I. Siddiqui, R. Ahmed, S.A. Chaudhry, Green synthesis of f-CdWO4 for photocatalytic degradation and adsorptive removal of Bismarck Brown R dye from water, Water Resour. Ind. 22 (2019) 100119.

[38] A.M. Priya, R.K. Selvan, B. Senthilkumar, M.K. Satheeshkumar, C. Sanjeeviraja, Synthesis and characterization of CdWO4 nanocrystals, Ceram. Int. 37 (7) (2011) 2485–2488.

[39] H. Kamani, S. Nasseri, M. Khoobi, R. Nabizadeh Nodehi, A.H. Mahvi, Sonocatalytic degradation of humic acid by N-doped TiO2 nano-particle in aqueous solution, Journal of Environmental Health Science and Engineering 14 (1) (2016) 3.

[40] S.H. Ali, Social and environmental impact of the rare earth industries, Resources 3 (1) (2014) 123–134.

[41] P. Seied Mahdi, R.-N. Mehdi, G. Mohammad Reza, K. Meisam Sadeghpour, N. Parviz, F. Farnoosh, Facile and effective synthesis of praseodymium tungstate nanoparticles through an optimized procedure and investigation of photocatalytic activity, Open Chemistry 15 (1) (2017) 129–138.

[42] K.-T. Rim, Effects of rare earth elements on the environment and human health: a literature review, Toxicol. Environ. Health Sci. 8 (3) (2016) 189–200.

[43] M.S. Roriz, J.F. Osma, J.A. Teixeira, S. Rodríguez Couto, Application of response surface methodological approach to optimise Reactive Black 5 decolouration by crude laccase from Trametes pubescens, J. Hazard. Mater. 169 (1) (2009) 691–696.

[44] M. Nie, Y. Yang, Z. Zhang, C. Yan, X. Wang, H. Li, W. Dong, Degradation of chloramphenicol by thermally activated persulfate in aqueous solution, Chem. Eng. J. 246 (2014) 373–382.

[45] C.-Y. Chen, Photocatalytic degradation of azo dye reactive orange 16 by TiO2, Water Air Soil Pollut. 202 (1) (2009) 335–342.

[46] S. Ahmadi, C.A. Igwegbe, Adsorptive removal of phenol and aniline by modified bentonite: adsorption isotherm and kinetics study, Appl. Water Sci. 8 (6) (2018) 170.

[47] S. Ahmadi, A. Banach, F. Mostafapour, D. Balarak, Study survey of cupric oxide nanoparticles in removal efficiency of ciprofloxacin antibiotic from aqueous solution: adsorption isotherm study, Desalin. Water Treat. 89 (2017) 297–303.

[48] S. Ahmadi, C.A. Igwegbe, S. Rahdar, The application of thermally activated persulfate for degradation of Acid Blue 92 in aqueous solution, Int. J. Ind. Chem. 10 (3) (2019) 249–260.

[49] J.X. Lu, J. Murray, Biochemistry, Dissolution and Solubility, StatPearls Publishing, Treasure Island (FL), USA, 2020.

[50] S. Ziembowicz, M. Kida, P. Koszelnik, Sonochemical formation of hydrogen Peroxide, Proceedings 2 (5) (2018) 188.

[51] S. Thangavel, N. Raghavan, G. Kadarkarai, S.-J. Kim, G. Venugopal, Graphene-oxide (GO)–Fe3+ hybrid nanosheets with effective sonocatalytic degradation of Reactive Red 120 and study of their kinetics mechanism, Ultrason. Sonochem. 24 (2015) 123–131.

[52] B. Gözmen, Applications of response surface analysis to the photocatalytic mineralization of acetaminophen over silver deposited Tio2 with periodate, Environ. Prog. Sustainable Energy 31 (2) (2012) 296–305.

[53] A. Khataee, M. Sheydaei, A. Hassani, M. Taseidifar, S. Karaca, Sonocatalytic removal of an organic dye using TiO2/Montmorillonite nanocomposite, Ultrason. Sonochem. 22 (2015) 404–411.

[54] A. Khataee, B. Kayan, P. Gholami, D. Kalderis, S. Akay, Sonocatalytic degradation of an anthraquinone dye using TiO2-biochar nanocomposite, Ultrason. Sonochem. 39 (2017) 120–128.

[55] D.F. Ollis, Kinetics of liquid phase photocatalyzed reactions: an illuminating approach, J. Phys. Chem. B 109 (6) (2005) 2439–2444.

[56] J.-T. Li, B. Bai, Y.L. Song, Degradation of Acid orange 3 in aqueous solution by combination of Fly ash/H2O2 and ultrasound irradiation, Indian J. Chem. Technol. 17 (2010) 198–203.

[57] S.K. Tang, T.T. Teng, A.F.M. Alkarkhi, Z. Li, Sonocatalytic degradation of rhodamine B in aqueous solution in the presence of Tio2 coated activated carbon, APCBEE Procedia 1 (2012) 110–115.

[58] N.F. Cardoso, R.B. Pinto, E.C. Lima, T. Calvete, C.V. Amavisca, B. Royer, M.L. Cunha, T.H.M. Fernandes, I.S. Pinto, Removal of remazol black B textile dye from aqueous solution by adsorption, Desalination 269 (1) (2011) 92–103.

[59] M.M. Baneshi, B. Naraghi, S. Rahdar, H. Azizabadi, M. Ahamadabadi, M.R. Narooie, A. Salimi, R. Khaksefidi, V. Alipour, Removal of remazol black B dye from aqueous solution by electrocoagulation equipped with iron and aluminium electrodes, IIOA3 J. 7 (2016) 529–535.

[60] A.R. Ziapour, M. Sefidrooh, M.R. Moadeli, Adsorption of Remazol Black B Dye from aqueous solution using bagasse, Progr. Color, Color. Coat. 9 (2) (2016) 99–108.

[61] K. Sudiana, I.D.K. Sastrawidana, I.N. Sukarta, Decolorization study of Remazol black B textile dye using local fungi of Ganoderma sp. and their ligninolytic enzymes, J. Environ. Sci. Technol. 11 (2018) 16–22.

[62] M. Aftab, A. Tahir, Biodegradation of Remazol black B by extracellular fungal laccase from Aspergillus oryzae AM1101, Int. J. Biosci. 13 (2018) 290–296.

[63] N. Firdous, I.A. Shaikh, R. Shahid, Decolorization of reactive azo dye remazol black b by using advanced oxidation processes (AOPs), J. Chem. Soc. Pak. 40 (2018) 828–833.

[64] S. Ahmadi, A. Rahdar, S. Rahdar, C. Igwegbe, Removal of Remazol Black B from solution aqueous using P-γ-Fe2O3 nanoparticles: synthesis, physical characterization, isotherm, kinetic, and thermodynamic studies, Desalin. Water Treat. 152 (2019) 401–410.

[65] H. Wang, J. Niu, X. Long, Y. He, Sonophotocatalytic degradation of methyl orange by nano-sized Ag/TiO2 particles in aqueous solutions, Ultrason. Sonochem. 15 (4) (2008) 386–392.

[66] L. Song, S. Zhang, X. Wu, Q. Wei, Synthesis of porous and trigonal TiO2 nanoflake, its high activity for sonocatalytic degradation of rhodamine B and kinetic analysis, Ultrason. Sonochem. 19 (6) (2012) 1169–1173.

[67] P.A. Soloman, C.A. Basha, M. Velan, V. Ramamurthi, K. Koteeswaran, N. Balasubramanian, Electrochemical degradation of remazol black B dye effluent, CLEAN – Soil Air, Water 37 (11) (2009) 889–900.